

Recognizing People by Body Shape Using Deep Networks of Images and Words

Blake A. Myers
The University of Texas at Dallas

Thomas M. Metz
The University of Texas at Dallas

Veda Nandan Gandhi
The University of Texas at Dallas

Alice J. O’Toole
The University of Texas at Dallas

Lucas Jaggernauth
The University of Texas at Dallas

Matthew Q. Hill
The University of Texas at Dallas

Carlos D. Castillo
Johns Hopkins University

Abstract

Common and important applications of person identification occur at distances and viewpoints in which the face is not visible or is not sufficiently resolved to be useful. We examine body shape as a biometric across distance and viewpoint variation. We propose an approach that combines standard object classification networks with representations based on linguistic (word-based) descriptions of bodies. Algorithms with and without linguistic training were compared on their ability to identify people from body shape in images captured across a large range of distances/views (close-range, 100m, 200m, 270m, 300m, 370m, 400m, 490m, 500m, 600m, and at elevated pitch in images taken by an unmanned aerial vehicle [UAV]). Accuracy, as measured by identity-match ranking and false accept errors in an open-set test, was surprisingly good. For identity-ranking, linguistic models were more accurate for close-range images, whereas non-linguistic models fared better at intermediary distances. Fusion of the linguistic and non-linguistic embeddings improved performance at all, but the farthest distance. Although the non-linguistic model yielded fewer false accepts at all distances, fusion of the linguistic and non-linguistic models decreased false accepts for all, but the UAV images. We conclude that linguistic and non-linguistic representations of body shape can offer complementary identity information for bodies that can improve identification in applications of interest.

1. Introduction

Studies of visually based person recognition have concentrated primarily on identity cues in the face because faces provide nearly unique information about identity.

Consistent with this axiom, behavioral studies indicate that when the entire person is visible, people rely strongly on the face [16], even when the body can be useful [15]. However, it is important in some cases, to identify people from distances and viewpoints that limit the resolution or visibility of the face. These types of vantage points are common in natural viewing environments and are typical for surveillance cameras that monitor large areas of space.

The use of bodies for identification in natural viewing conditions is possible because body identity cues (e.g., shape, structure of body) remain visible and easy to resolve across a large range of distances. Concomitantly, behavioral studies indicate that people rely on bodies when the face is not easy to see [5] or provides poor or misleading information about identity [15, 14]. Although the identity cues from the body are inherently less diagnostic than cues from the face, they can nonetheless support surprisingly accurate identification for human perceivers, both in isolation [5, 15, 14, 16] and in combination with other visually robust biometrics such as gait [8, 23]. Thus, the use of body identity information as a component of biometric fusion (e.g., face, body, and gait) offers the possibility of improving person recognition in challenging viewing conditions.

In this study, we examined the extent to which body shape can support accurate identification. We distinguish this problem from the more commonly studied *person re-identification* problem, which “aims to retrieve a person of interest across multiple non-overlapping cameras” (see [22] for a review). Although the body is used extensively in re-identification, many “identity” cues that operate at this short time scale (e.g., clothing, footwear, hairstyle, accessories) cannot be relied upon over a longer time period. In eliminating these short-term cues, the shape and structure of the body remain the primary cues to identity.

Table 1. Linguistic descriptors used to annotate frames.

proportioned	rectangular	stocky
short legs	muscular	average
tall	sturdy	big
long legs	lean	short torso
pear-shaped	petite	broad shoulders
heavy set	long	long torso
round (apple)	built	fit
skinny	masculine	small
pear-shaped	petite	broad shoulders
short	feminine	curvy

Person identification using body shape is challenging for multiple reasons. First, the human body is a three-dimensional object capable of both rigid and non-rigid deformation. Bodies can appear from multiple views, with limbs in any number of configurations or poses (e.g., arms up, leg lifted). Second, changes in clothing can alter the color and texture of the body in unpredictable ways. This is a challenging problem in light of multiple findings indicating that the most commonly employed machine learning algorithms (i.e., deep convolutional neural networks [DCNNs]) show a strong texture bias in classification, with less sensitivity to the global shape of an object (cf. [3]).

Third, high-quality datasets available for training body recognition algorithms across diverse viewpoints, distances, and appearances (e.g., clothing) are quite limited. This makes it difficult to use training diversity to overcome the texture bias problem and other types of over-fitting.

Our approach combines elements of a standard image-based deep network with a body representation trained to produce a description of the body based on a small number ($n = 30$) of linguistic attributes (cf. [7, 18] and Table 1). Human-annotated linguistic descriptors (e.g., words such as curvy, pear-shaped, muscular, and broad shoulders) offer advantages for body shape representations, because they are accessible and constant over a wide range of viewing distances, angles, clothing, and footwear. A “curvy woman” or “muscular, broad-shouldered” man can be perceived and annotated easily over photometric change. Moreover, each word can entail multiple global and local anthropometric features. For example, the word “pear-shaped” indicates large hips relative to bust size and suggests a bottom-heavy body shape. Combinations of these words are even more powerful in conjuring up the gross shape of a body. We can imagine a tall, muscular, athletic, broad-shouldered man quite easily, and distinguish this body shape from other types of athletic, muscular bodies (e.g., cyclist, rock climber) [7, 18].

The contributions of the paper are:

- Proposal of a body identification algorithm that uses



Figure 1. Example image frames from the BRS dataset that show two identities from multiple viewpoints.

a combination of object recognition strategies and linguistic body descriptions.

- Direct comparisons between models pre-trained with and without a linguistic core.
- Evaluation of the algorithms across a broad range of distances (close-up, 100m, 200m, 270m, 300m, 370m, 400m, 490m, 500m, 600m), viewpoints, and at elevated pitches from a UAV.
- Demonstration that the performance of linguistic and non-linguistic models differs at different distances, and with UAV.
- Demonstration that fusing linguistic and non-linguistic models can improve body identification over either linguistic or non-linguistic core models operating alone.
- Novel body shape algorithms that operate in challenging testing conditions (mismatched clothing, long-distances, difficult viewing angles).

1.1. Related Work

Body Shape Identification. Work using body shape as a biometric is surprisingly limited. In one early paper [4], 73 human-placed anthropometric landmarks from bodies in the Civilian American and European Surface Anthropometry Resource [CAESAR] dataset were used as a body shape representation. CAESAR is a database with 5000+ 3D laser scans of American and European adults. The utility of these landmarks for identity verification was tested for a gallery set of original anthropometric measures and a probe set consisting of noise-perturbed versions of the gallery. Although the model performed well, the landmark measures are useful only when they are available with 3D body models.

In metric terms, body measures including height and weight have been used as body biometrics in forensic scenarios. In using a 3D model to estimate these quantities, height and weight were estimated accurately for a wide range of body poses and camera angles when a 3D model

can be reliably determined [20]. However, scale disambiguation was not feasible in real-world scenarios with coherent point drift (CPD) [11]. Thus, the authors concluded that “3D pose estimation” is necessary, but not sufficient, to achieve accurate estimates of height and weight.

In a subsequent study [21], height and weight were estimated using pose estimation software that relies on creating an underlying 3D model of a person from an image. SMPLify-X [13] an extended version of the SMPL model [9] was employed. SMPL is a principal components model of laser scans of human bodies [10]. From 2D detected keypoints, 3D body parameters (pose θ , shape β , and expression ψ) were estimated by minimizing the difference between the 2D keypoints and the 3D keypoints reprojected into the image plane. Weight estimates for above- and below-average sized bodies were poor. Including 2D silhouette information improved estimates.

In another approach, a data-driven strategy was used to test scale agnostic body shape classification for large numbers of 3D body models synthesized from sampled SMPL β parameters [21]. Equivalence classes (19 for female bodies, and 15 for male bodies—manually narrowed to 12 categories each) were found. The model was evaluated for reliability in estimating height, weight, and non-metric categorization of 3D shapes using a scale-agnostic measure of body shape. Although the approach improves on previous efforts [20], accurate body-shape identification using 3D models created from a single, reference-free image remains challenging.

Linguistic Descriptions for Body Synthesis. Our use of linguistic descriptors as a body biometric was inspired by two studies [7, 18]. Both demonstrate that it is possible to reconstruct a perceptually and metrically accurate three-dimensional model of a person’s body by learning the mapping between 30 linguistic attributes (see Table 1) and the β coefficients from the SMPL model. We reasoned that if these 30 linguistic attributes were useful in reconstructing an accurate body model, they might also serve as a useful representation of body shape that could be used to identify, or at least classify bodies by shape.

The problem we undertake requires learning a mapping from 2D images of a body to the linguistic descriptor terms. The goal of the present work was to use the descriptor-based representation as part of a core ResNet101 model that could be refined by explicitly using transfer learning to train the model for identification.

2. Experiments

We conducted experiments to test the role of linguistic features in identification of people by body shape. A model trained to predict a word-based description (see Table 1) of a human body served as the core ResNet model for the linguistic model. The model was then trained with transfer

learning to identify people by body. This linguistic model was compared to an otherwise identical model without linguistic training.

2.1. Datasets

Linguistic Training. Training of the linguistic core was done with annotations of identities using single frames extracted from two data sets: the Human Identification (HumanID) [12], and the Multiview Extended Video with Activities (MEVA) datasets [2]. For the former, three types of videos were sampled: a.) people approaching from a distance, b.) people passing perpendicular to a camera, and c.) people viewed from an approximately 45° raised pitch. Annotations were collected on each of the 297 identities available in the dataset from 20 annotators. Specifically, annotations were collected from (all/most) frames in which a body could be detected, yielding a total of approximately (250K) frames. These frames were annotated with the 30 linguistic descriptors listed in Table 1. Descriptors for each identity were averaged across annotators and the averages were used for training. The network learned to produce the descriptors from the images.

The MEVA dataset [2] is a very-large-scale dataset for human activity recognition. It contains over 9,300 hours of untrimmed video, loosely scripted to include a diverse range of activities and background scenes. There are 37 activity types performed by approximately 100 actors in scripted scenarios. Human ratings were gathered on all 158 available identities in the dataset. Because no explicit identity labels were provided in the MEVA dataset, images were cropped out of the 7,000 available videos and annotated by between 11–15 annotators. Again, the network was trained to produce the descriptors from the images.

Identification Transfer Training. To train and evaluate models, we used the BRIAR dataset [1], which is divided into a training (BRIAR Research Set, BRS) and a test set (BRIAR Test Set, BTS). These sets were issued in multiple releases, which included increasing numbers of identities. The BRS was used for identification transfer training, and a curated subset of BTS was used for testing (see Section 2.3 for details of this dataset).

For training, we utilized BRS1–3 (See Table 2). For each subject, there are indoor (controlled) and outdoor (field) sequences. In the controlled set, cameras captured walking videos of two types: structured walking and random walking. In addition to the walking types, there were also standing videos. All distances except for the close-range set had one viewing angle, whereas the close-range set had three cameras capturing the same position from different yaw angles: 0°, 30°, and 50°. All sequences involved two clothing settings. Example identities appear in Figure 1. Examples of images taken at different distance conditions and from UAV appear in Figure 2.

Training	IDs	Images	Distance & Pitch (UAV)				
BRS1	158	46834	100m	200m	400m	500m	UAV
BRS1.1	54	13288	100m	300m	400m	500m	UAV
BRS2	195	51134	100m	270m	370m	800m	1000m
BRS3	170	88573	100m	200m	300m	500m	

Table 2. Training data subsets indicating number of identities and distances in meters. UAV refers to image frames in video taken from an unmanned aerial vehicle.



Figure 2. Example images of one identity at each distance in the BRS1 dataset.

2.2. Model Components

We created two identity-trained models that differed only in the base model to which identity transfer learning was applied. We refer to these as the Linguistic Core ResNet Identity Model (LCRIM) and the Non-Linguistic Core ResNet Identity Model (NLCRIM). A fusion model was created by combining the results of the LCRIM and NLCRIM models. Specifically, cosine similarities for all possible probe-gallery pairs were computed for both the LCRIM and NLCRIM models. The average of the two cosines served as the representation for the fusion model.

Linguistic and Non-linguistic Core Training. The *linguistic core* model derives from a ResNet-101 architecture. Specifically, the model consists of a base ResNet 101 [6] pre-trained with ImageNet [17]. Transfer learning was applied to the base model to map from image frames in the MEVA and HumanID datasets (see Section 2.1) to the 30 linguistic body attributes (see Table 1). The architecture of the final model consisted of the ResNet base with an ap-

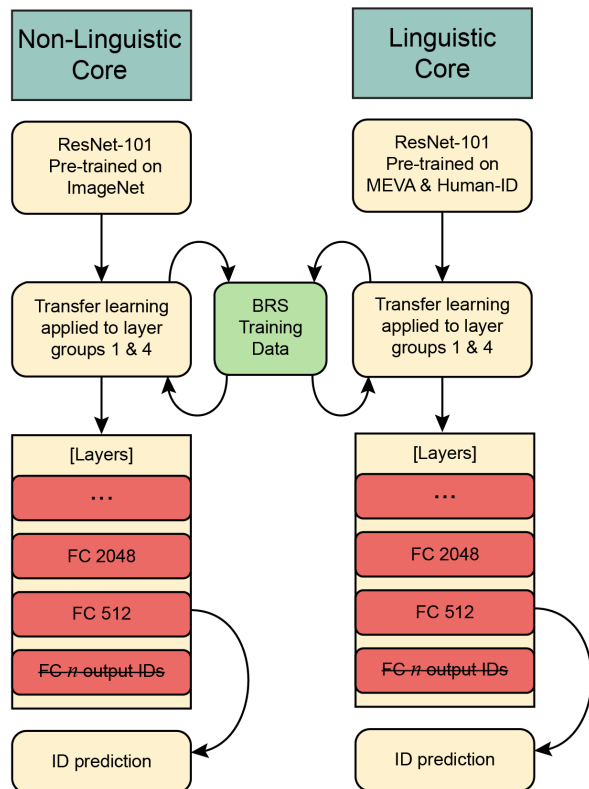


Figure 3. Model architecture with image core (left) and linguistic core (right). Both are trained for identification using image frames from BRS. “Layer groups” refer to network subdivisions used by the code implementation (see text).

Distance	Gallery IDs	Probe IDs	Probe Images
Close Range	60	95	1353
100m–300m	60	86	638
370m–600m	60	92	1354
UAV	60	17	204

Table 3. BTS dataset used for model evaluation as a function of distance/view. In this dataset, there are more unique probe identities ($n = 100$) than unique gallery identities ($n = 60$) making this an open-set test.

pended encoder ($2048 \rightarrow 512 \rightarrow 64 \rightarrow 16$) to a decoder ($16 \rightarrow 24 \rightarrow 30$). The *non-linguistic core* model was simply the base ResNet 101 [6] pre-trained with ImageNet [17].

Identification Transfer Learning for Bodies. Both net-

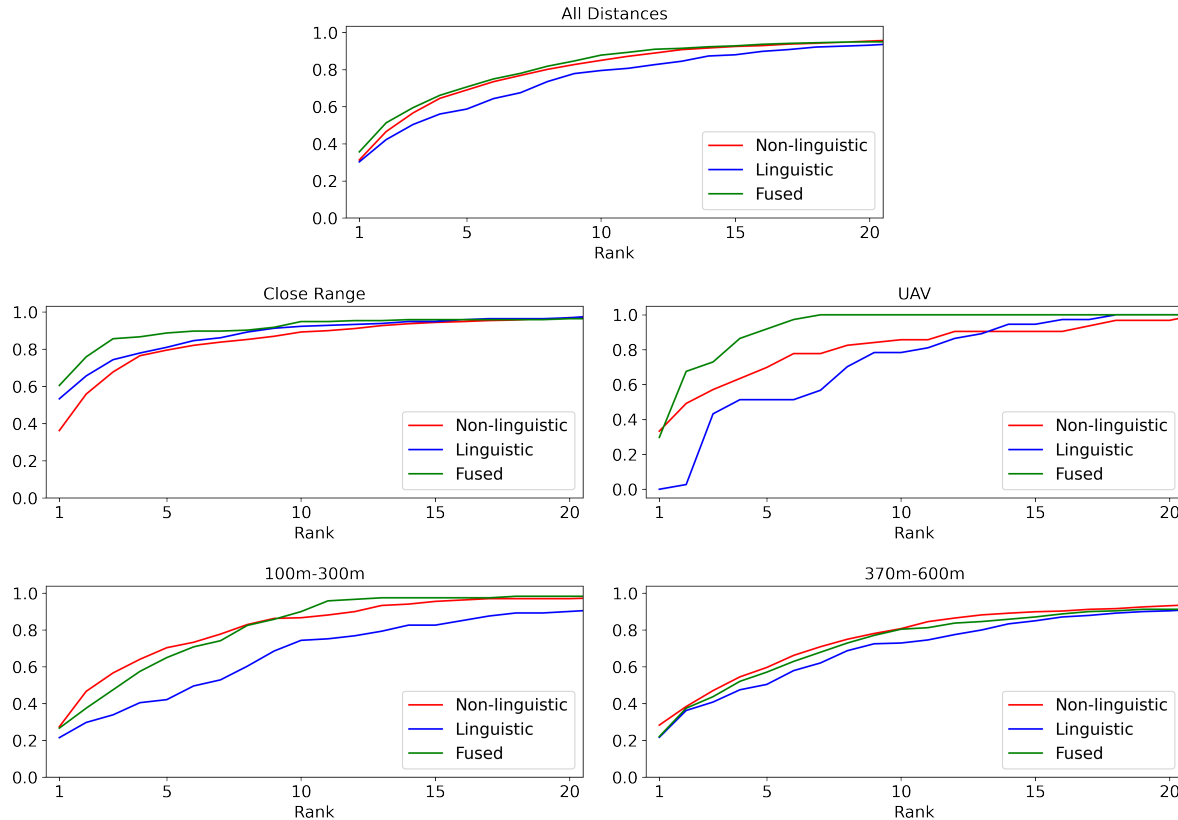


Figure 4. Cumulative Match Characteristic (CMC) curves comparing the performance of the Linguistic (LCRIM) and Non-Linguistic Core ResNet Identity models (NLCRIM), plotted with the fusion of the models. At close range, the linguistic model performed more accurately across all ranks. The non-linguistic model fared better at intermediary distances. Notably, fusion of the two model embeddings was helpful in most cases, regardless of whether the linguistic or non-linguistic model performed more accurately.

works consist of core models (linguistic, non-linguistic) that were altered via transfer learning for identification (i.e., separating individual people by identity). This learning was applied to the first and fourth network layer groups. Here, “layer groups” refer to the five subsections of the ResNet architecture used in the PyTorch implementation and detailed in Table 2 of [6]. These layer groups each consist of multiple residual blocks. To adapt the ResNet 101 for body identification, identity training was implemented using still images for each identity, as well as image frames extracted from the BRS1–3 videos. Image frame extraction was done by partitioning video frames into equal-length groupings and randomly selecting 5 frames across the video partitions. Image crops were then generated with a pre-trained Inception-Net-V2 object detector [19]. Low-confidence crops were discarded to assure high-quality crops. This frame selection method generated a total of 199,829 images of 577 identities across the distances and views available in BRS (see Table 2).

We pre-processed the dataset by resizing the images to 128x256 pixels (retaining aspect ratio) and normalizing the

pixel values. The dataset was split into training and validation sets in a ratio of 80:20. The model was trained using the cross-entropy loss function and the Adam optimizer with a starting learning rate of 0.00005 and momentum of 0.9. We used flipping and rotation as data augmentation techniques. The end part of the model architecture was an Adaptive Average Pooling layer, followed by a fully connected layer with 2048 input features and 512 output features. A Parametric Rectified Linear Unit (PReLU) activation function was then applied. Lastly, a sequential block containing a fully connected layer mapped the 512 input features to the 577 identities on which the model was trained.

2.3. Model Evaluation

Test Data. Test data from the BTS are summarized in Table 3. The gallery consisted of both images and videos. The probe set consisted of videos only. In all cases, matched-identity gallery and probe items wore different clothes. For gallery items, images were processed through both networks to produce a feature-embedding for each network. These embeddings were extracted from the

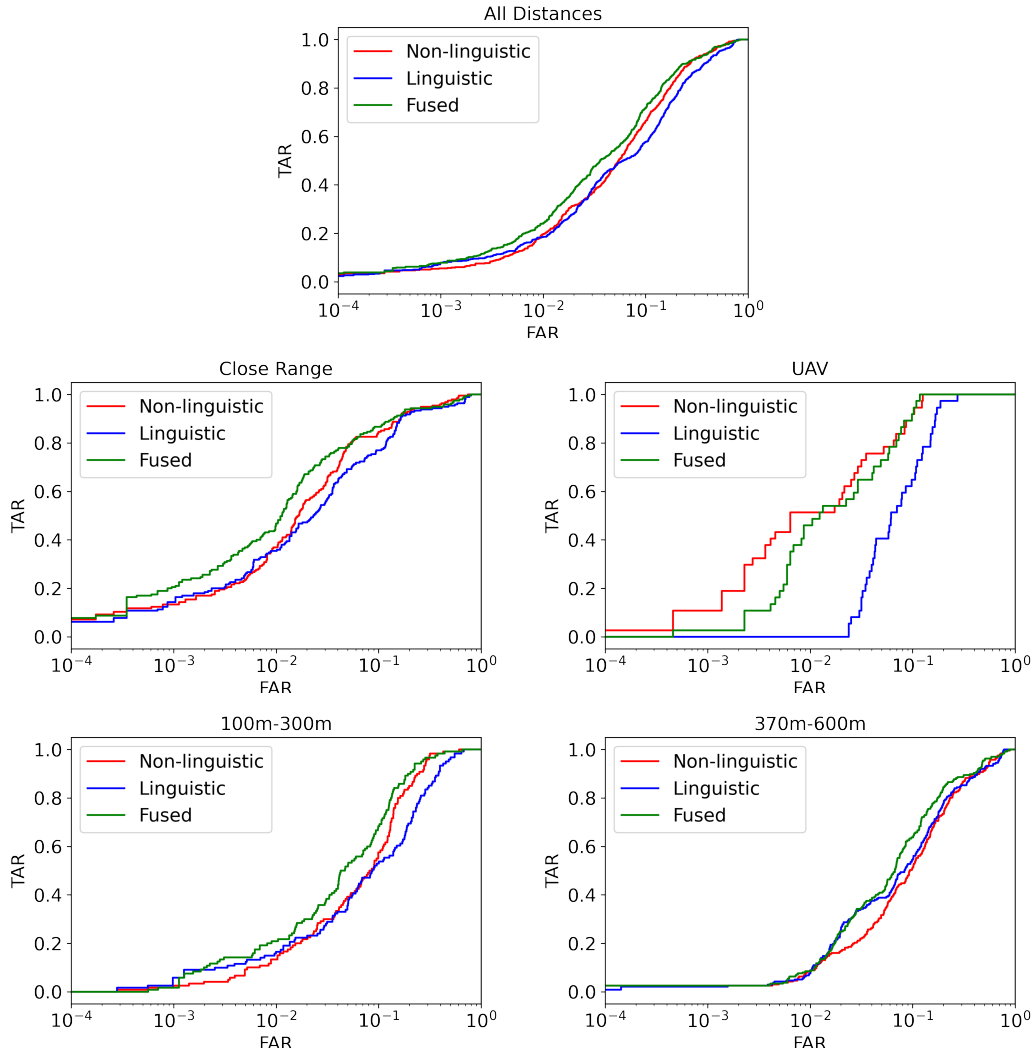


Figure 5. Receiver Operating Characteristic (ROC) curves comparing the performance of the Linguistic (LCRIM) and Non-Linguistic Core ResNet Identity models (LCRIM), plotted with the fusion of the models. Although the non-linguistic model fared better in all cases, the fusion of the two model embeddings improved performance for all cases, with the exception of the UAV. (True accept rate, TAR; False accept rate, FAR)

penultimate layer of each network (512 units). For each gallery identity, the feature vectors from the images and videos were averaged to produce a single representation for each unique identity.

For both the gallery and probe videos, every sixth frame was extracted. These frames were processed through both networks to produce feature embeddings, again extracted from the penultimate layer of 512 units. A single representation of the video was made by averaging the features for the extracted frames.

Quantitative Evaluation Procedure. Model testing was implemented as a 1-to-1 verification between gallery and probe items, with cosine as the similarity metric. Performance was analyzed in two ways. Cumulative Match

Characteristic (CMC) curves show the proportion of correctly matched items as a function of the rank of the match. Receiver Operating Characteristic (ROC) curves show the true accept rate as a function of the false accept rate. This latter curve is particularly useful for examining model performance in the open set case, where the number of unique gallery identities is less than unique probes identities.

Ranked Match Results. The CMC results appear in Figure 4 and show data for the three models, NLCRIM, LCRIM, and Fused. Each plot shows CMC curves displayed by the condition: Close Range, UAV, 100m–300m, and 370m–600m, and averaged across all conditions (All Distances). Table 4 gives the proportion of correct identifications at Rank 1, 10, and 20 by distance condition and as

Model	All Distances			Close Range			UAV			100m–300m			370m–600m		
NLCRIM	0.31	0.85	0.95	0.36	0.89	0.97	0.33	0.86	0.97	0.27	0.87	0.97	0.28	0.81	0.93
LCRIM	0.30	0.80	0.93	0.53	0.92	0.97	0.00	0.78	1.00	0.21	0.74	0.90	0.22	0.73	0.90
Fused	0.36	0.88	0.95	0.61	0.95	0.96	0.30	1.00	1.00	0.27	0.90	0.98	0.22	0.80	0.91

Table 4. Performance as the proportion of probe items correctly matched to their gallery identity at rank 1, rank 10, and rank 20. Fusion improves most categories of items.

summarized over all distances.

Identification performance was surprisingly accurate. As the table shows, across all distances in the fused model, 36% of the probe items with a matched identity in the gallery were matched at Rank 1, 88% were matched by Rank 10, and 95% were matched by Rank 20. Figure 4 shows that the Fused model was slightly, but consistently, superior to the NLCRIM and LCRIM models at all ranks. This indicates that models with and without a linguistic core contain complementary information for body identification that can be combined to improve performance. That conclusion is supported by the rank data in Table 4. At Rank 1, 10, and 20, fusion yields the best performance obtained at these ranks.

Dividing the data by category, Figure 4 and Table 4 show that the LCRIM model performed more accurately than NLCRIM in the close-range condition, whereas NLCRIM was more accurate in the other conditions (100–300m, 370–600m, UAV). The fused model fared better than both the LCRIM and NLCRIM for the close range and UAV data. For distances between 100 and 300m, fusion dominated only at ranks greater than 10. Not surprisingly, the poorest performance for all models was found for distances between 370 and 600m. In this condition, the NLCRIM, rather than the Fused model, performed best.

The UAV condition is of special interest. Despite the strong superiority of the NLCRIM over the LCRIM, and the relatively weak performance of the LCRIM, fusion improved performance by a large margin at all ranks—with the fused model reaching 100% correct matches by Rank 10. This indicates the utility of combining these two sources of information about bodies with extreme overhead pitch.

Verification Rate Results. The ROC results appear in Figure 5 and provide an evaluation of the models’ performance across various operating points. The ROC is especially important because it includes false match error for probe items that do not have a matching gallery entry. These results complement the CMC analysis but offer additional information about the challenges of the open set problem.

To begin, as for the CMC data, the ROC results show a small, but consistent, benefit from fusing the LCRIM and NLCRIM models across a wide swath of false accept rates. The advantage of fusion was consistent across false accept rates for the close range and 100–300m conditions, and across some but not all false accept rates in the 370–600m condition. Contrary to the fusion advantage seen with the

CMC measure, using the ROC measure, fusion did not benefit the UAV category. Instead, the NLCRIM model performed best.

In examining the NLCRIM and LCRIM models by themselves, neither showed a clear and consistent advantage over the other at all ranks. This further emphasizes the potential for a benefit of fusion across different conditions and different operating points of the model.

3. Discussion

A key challenge in person identification using body shape is the considerable variability in appearance due to changes in clothing, viewpoint, and distance. The limited availability of high-quality datasets for training body recognition algorithms exacerbates these challenges. We addressed these issues by employing a combination of object recognition strategies and linguistic body descriptions, with the idea that linguistic descriptions might be more robust to changes in appearance and might instead rely more fundamentally on body shape for identification.

The approach began with a deep network trained to predict linguistic descriptors of body shape. Transfer learning was applied to train this core network to identify people based on body images. We compared the performance of this linguistic model with that of an identical model without linguistic training. The models were evaluated with a diverse test set comprised of images and videos taken over a wide variety of distances and from an elevated pitch.

The linguistic and non-linguistic models performed surprisingly well at body identification. This suggests that there may be more identity-diagnostic information in bodies than previously assumed. As expected, body identification was best at close distances, but remained relatively robust with hundreds of meters of distance and from elevated pitch (UAV). Given that body shape is not a unique biometric, this result has important implications. Person identification can be critical in cases where the face is not visible or resolvable, the possibility of relying on body information, either in isolation or in combination with gait.

The utility of fusing different kinds of information from static bodies for body identification was evident. A fusion of the linguistic and non-linguistic models improved body identification in most cases. The proposed method operated effectively in demanding testing conditions, including at a distance, with overhead viewing, and with mis-

matched clothing. This highlights the potential of the approach for applications in security and surveillance, where person identification often relies on distant and obstructed views of the subject.

In conclusion, we demonstrate the feasibility of body shape for person identification, using a novel approach that leverages linguistic body descriptions with an object classification approach. The fusion of linguistic and non-linguistic information can improve body identification, offering a promising direction for future research and practical applications in challenging viewing conditions.

References

- [1] D. Cornett, J. Brogan, N. Barber, D. Aykac, S. Baird, N. Burchfield, C. Dukes, A. Duncan, R. Ferrell, J. Goddard, et al. Expanding accurate person recognition to new altitudes and ranges: The briar dataset. In *Proceedings of the IEEE/CVF Winter Conference on Applications of Computer Vision*, pages 593–602, 2023.
- [2] K. Corona, K. Osterdahl, R. Collins, and A. Hoogs. Meva: A large-scale multiview, multimodal video dataset for activity detection. In *Proceedings of the IEEE/CVF Winter Conference on Applications of Computer Vision (WACV)*, pages 1060–1068, January 2021.
- [3] R. Geirhos, P. Rubisch, C. Michaelis, M. Bethge, F. A. Wichmann, and W. Brendel. Imagenet-trained cnns are biased towards texture; increasing shape bias improves accuracy and robustness. *arXiv preprint arXiv:1811.12231*, 2018.
- [4] A. Godil, P. Grother, and S. Ressler. Human identification from body shape. In *Fourth International Conference on 3-D Digital Imaging and Modeling, 2003. 3DIM 2003. Proceedings.*, pages 386–392. IEEE, 2003.
- [5] C. A. Hahn, A. J. O’Toole, and P. J. Phillips. Dissecting the time course of person recognition in natural viewing environments. *British Journal of Psychology*, 107(1):117–134, 2016.
- [6] K. He, X. Zhang, S. Ren, and J. Sun. Deep residual learning for image recognition, 2015.
- [7] M. Q. Hill, S. Streuber, C. A. Hahn, M. J. Black, and A. J. O’Toole. Creating body shapes from verbal descriptions by linking similarity spaces. *Psychological science*, 27(11):1486–1497, 2016.
- [8] A. Kale, A. Sundaresan, A. Rajagopalan, N. P. Cuntoor, A. K. Roy-Chowdhury, V. Kruger, and R. Chellappa. Identification of humans using gait. *IEEE Transactions on image processing*, 13(9):1163–1173, 2004.
- [9] M. Loper, N. Mahmood, J. Romero, G. Pons-Moll, and M. J. Black. Smpl: A skinned multi-person linear model. *ACM transactions on graphics (TOG)*, 34(6):1–16, 2015.
- [10] M. Loper, N. Mahmood, J. Romero, G. Pons-Moll, and M. J. Black. Smpl: A skinned multi-person linear model. *ACM Trans. Graph.*, 34(6), nov 2015.
- [11] A. Myronenko and X. Song. Point set registration: Coherent point drift. *IEEE transactions on pattern analysis and machine intelligence*, 32(12):2262–2275, 2010.
- [12] A. O’Toole, J. Harms, S. Snow, D. Hurst, M. Pappas, J. Ayyad, and H. Abdi. A video database of moving faces and people. *IEEE Transactions on Pattern Analysis and Machine Intelligence*, 27(5):812–816, 2005.
- [13] G. Pavlakos, V. Choutas, N. Ghorbani, T. Bolkart, A. A. Osman, D. Tzionas, and M. J. Black. Expressive body capture: 3d hands, face, and body from a single image. In *Proceedings of the IEEE/CVF conference on computer vision and pattern recognition*, pages 10975–10985, 2019.
- [14] A. Rice, P. J. Phillips, V. Natu, X. An, and A. J. O’Toole. Unaware person recognition from the body when face identification fails. *Psychological Science*, 24(11):2235–2243, 2013.
- [15] A. Rice, P. J. Phillips, and A. O’Toole. The role of the face and body in unfamiliar person identification. *Applied Cognitive Psychology*, 27(6):761–768, 2013.
- [16] R. A. Robbins and M. Coltheart. The effects of inversion and familiarity on face versus body cues to person recognition. *Journal of Experimental Psychology: Human Perception and Performance*, 38(5):1098, 2012.
- [17] O. Russakovsky, J. Deng, H. Su, J. Krause, S. Satheesh, S. Ma, Z. Huang, A. Karpathy, A. Khosla, M. Bernstein, et al. Imagenet large scale visual recognition challenge. *International journal of computer vision*, 115:211–252, 2015.
- [18] S. Streuber, M. A. Quiros-Ramirez, M. Q. Hill, C. A. Hahn, S. Zuffi, A. O’Toole, and M. J. Black. Body talk: Crowd-shaping realistic 3d avatars with words. *ACM Transactions on Graphics (TOG)*, 35(4):1–14, 2016.
- [19] C. Szegedy, S. Ioffe, V. Vanhoucke, and A. Alemi. Inception-v4, inception-resnet and the impact of residual connections on learning. In *Proceedings of the AAAI conference on artificial intelligence*, volume 31, 2017.
- [20] N. Thakkar and H. Farid. On the feasibility of 3d model-based forensic height and weight estimation. In *Proceedings of the IEEE/CVF Conference on Computer Vision and Pattern Recognition*, pages 953–961, 2021.
- [21] N. Thakkar, G. Pavlakos, and H. Farid. The reliability of forensic body-shape identification. In *Proceedings of the IEEE/CVF Conference on Computer Vision and Pattern Recognition (CVPR) Workshops*, pages 44–52, June 2022.
- [22] M. Ye, J. Shen, G. Lin, T. Xiang, L. Shao, and S. C. Hoi. Deep learning for person re-identification: A survey and outlook. *IEEE transactions on pattern analysis and machine intelligence*, 44(6):2872–2893, 2021.
- [23] G. Yovel and A. J. O’Toole. Recognizing people in motion. *Trends in cognitive sciences*, 20(5):383–395, 2016.

4. Acknowledgements

This research is based upon work supported in part by the Office of the Director of National Intelligence (ODNI), Intelligence Advanced Research Projects Activity (IARPA), via [2022-21102100005]. The views and conclusions contained herein are those of the authors and should not be interpreted as necessarily representing the official policies, either expressed or implied, of ODNI, IARPA, or the U.S.

Government. The US. Government is authorized to reproduce and distribute reprints for governmental purposes notwithstanding any copyright annotation therein.